



Computation of 3D coastal hydrodynamics through the vortex force formalism implemented by coupling TOMAWAC and TELEMAC-3D

Maria João Teles, Thierry Fouquet, Antonio Pires-Silva, Michel Benoit

► To cite this version:

Maria João Teles, Thierry Fouquet, Antonio Pires-Silva, Michel Benoit. Computation of 3D coastal hydrodynamics through the vortex force formalism implemented by coupling TOMAWAC and TELEMAC-3D. XXVIth Telemac & Mascaret User Club, Oct 2019, Toulouse, France. hal-02568536

HAL Id: hal-02568536

<https://hal.science/hal-02568536>

Submitted on 9 May 2020

HAL is a multi-disciplinary open access archive for the deposit and dissemination of scientific research documents, whether they are published or not. The documents may come from teaching and research institutions in France or abroad, or from public or private research centers.

L'archive ouverte pluridisciplinaire **HAL**, est destinée au dépôt et à la diffusion de documents scientifiques de niveau recherche, publiés ou non, émanant des établissements d'enseignement et de recherche français ou étrangers, des laboratoires publics ou privés.

Computation of 3D coastal hydrodynamics through the vortex force formalism implemented by coupling TOMAWAC and TELEMAC-3D

Maria João Teles, Thierry Fouquet
LNHE, EDF R&D
Chatou, France
maria.teles@edf.fr, thierry.fouquet@edf.fr

Antonio Pires-Silva
IST, University of Lisbon
Lisbon, Portugal

Michel Benoit
Institut de Recherche sur les Phénomènes Hors-Equilibre
(Irphé - UMR 7342)
Aix Marseille Univ., CNRS, Centrale Marseille
Marseille, France

Abstract — The implementation of the new TELEMAC-3D-TOMAWAC coupled system [5] on the latest TELEMAC-MASCARET version (v8p1) is presented. The new coupled system, based on a vortex-force formalism [7] is applied on a barred beach test case. The improvement of three-dimensional wave-current interaction effects on the hydrodynamics description is evidenced.

I. INTRODUCTION

The coastal domain is a complex hydrodynamic system where physical phenomena with different time and space scales interact. This is the case of waves and currents interaction.

The wave breaking process together with wave-induced currents can create a dangerous environment for swimmers and have a great impact on morphodynamics in the nearshore areas. Depending on the bottom morphology and on the incident wave field, currents can have different characteristics. If obliquely incident waves break on a alongshore uniform planar beach, a longshore current is generated. If the beach has, for example, sand bars or cusps, rip currents can be generated.

The wave-current environment is well described in a 2DH framework by the work of [1], through the radiation stress concept, already implemented by coupling the hydrodynamic model TELEMAC-2D [2] and spectral wave modelling TOMAWAC [3]. A couple of years ago, this approach was extended to TELEMAC-3D code assuming a uniform distribution of the radiation stresses over depth. Therefore the vertical structure of the flow was not properly assessed.

Nevertheless the three-dimensional (3D) structure of the flow can give relevant information about sediment transport, linked to the value of the velocities near the bottom, or to assess wave power availability at a certain location.

During the PhD thesis of Teles [4], [5] a new TELEMAC-3D - TOMAWAC coupling system was developed, based on a vortex force formalism.

The theoretical framework chosen was the glm2z-RANS [7] equations. To do so, the three-dimensional TELEMAC-3D equations were modified together with new boundary conditions and new parametrizations were included in TOMAWAC to calculate the wave forcing terms.

The purpose of this paper is to present the implementation of the developed TELEMAC-3D - TOMAWAC coupled system [4], [5] on the latest TELEMAC-MASCARET version (v8p1). The improvement of wave-current interaction effects on the 3D hydrodynamics description is evidenced.

In the following section a brief description of the new wave forcing terms included in TOMAWAC and the modified equations implemented on TELEMAC-3D is given together with the new key-words created in the steering file to activate this coupling mode.

In section III, a barred beach test case is used to analyse the vertical structure of the flow, followed by section IV, where some concluding remarks and perspectives are given.

II. COUPLING SYSTEM

A. Governing equations

To take into account the 3D effects of the combined environment the mathematical framework proposed by [7], the glm2z-RANS equations, was implemented. Following [8] the vertical current shear was neglected in the wave forcing terms.

The wave forcing terms are calculated in new fortran subroutines created in TOMAWAC model, namely:

- The momentum lost by waves from bottom induced wave breaking, through the variables FDX, FDY, calculated in fdiss3d.f;
- The momentum lost by waves due to bottom friction, through the variables FBX, FBY calculated in fbott3d.f;
- The wave enhanced mixing (v_{wz}), with the variable FDK, calculated in fdissk.f;
- The bottom friction modified from the wave-current environment, with the variable CFW, calculated in fric3d.f;
- The Stokes drift (U_{as}), through the variables UST, VST, calculated in uvstokes.f
- The wave induced pressure (J), with the variable WIP, calculated in wipj.f
- The momentum lost by waves due to white-capping together with the input momentum transferred from wind to the wave field, with variables FWX, FWY, calculated in moudiss.f and windiss.f.

These new terms are transferred to TELEMAC-3D model by means of source/sink terms on the mass (1) and momentum (2) conservation equations, and boundary conditions. Considering an incompressible fluid and the hydrostatic assumption, the new equations become:

$$\frac{\partial \hat{u}_\alpha}{\partial x_\alpha} + \frac{\partial \hat{w}}{\partial z} = 0 \quad (1)$$

$$\frac{\partial \hat{u}_\alpha}{\partial t} + \hat{u}_\beta \frac{\partial \hat{u}_\alpha}{\partial x_\beta} + \hat{w} \frac{\partial \hat{u}_\alpha}{\partial z} = S_\alpha - g \frac{\partial \hat{\eta}}{\partial x_\alpha} + \frac{\partial}{\partial x_\beta} \left(v_H \frac{\partial \hat{u}_\alpha}{\partial x_\beta} \right) + \frac{\partial}{\partial z} \left((v_z + v_{wz}) \frac{\partial \hat{u}_\alpha}{\partial z} \right) - \epsilon_{\alpha\beta\gamma} (f_3 + \omega_3) U_{\beta s} - W_s \frac{\partial \hat{u}_\alpha}{\partial z} - \frac{\partial J}{\partial x_\alpha} \quad (2)$$

$(\hat{u}_\alpha, \hat{w})$ represent the quasi-Eulerian velocities ($\alpha = 1, 2$ corresponding to horizontal coordinates), defined in a second order theory approach, by the difference between the Lagrangian mean velocities and the Stokes drift (U_{as}, W_s). S_α represents the hydrodynamic model horizontal source or sink terms of momentum, for instance, the Coriolis force. The acceleration due to gravity is given by g , and $S_{x\alpha}$ represent the hydrodynamic model horizontal source terms, for instance, the Coriolis force. v_H and v_z are, respectively, the horizontal and vertical turbulence viscosities. The viscosity values can either be prescribed by the user or computed by a turbulence closure model. Furthermore, within the wave-current environment and due to wave breaking there is an enhancement of the vertical mixing. To take account of this effect, the approach proposed by [12] was followed by adding the wave-enhanced vertical mixing, v_{wz} to the vertical turbulence viscosity v_z :

$$v_{wz}(z) = c_b Q_{br} \frac{1}{\sqrt{2}} \frac{H_s}{\sqrt{2}} D f^{wb}(z) \quad (3)$$

with :

$$f^{wb}(z) = \frac{1 - \tanh[k_b(\hat{\eta} - z)^2]}{\int_{-h}^{\hat{\eta}} (1 - \tanh[k_b(\hat{\eta} - z)^2]) dz} \quad (4)$$

Q_{br} represents the wave breaking sink term, D the total depth and $k_b = \frac{\sqrt{2}}{a_b H_s}$, with $a_b = 1.2$ and $c_b = 0.03$.

The vortex force in x_α direction, which is represented in $\epsilon_{\alpha\beta\gamma} (f_3 + \omega_3) U_{\beta s}$, is defined by the vectorial product between the mean flow vertical vorticity ω_3 and the horizontal Stokes drift $U_{\beta s}$. The Stokes-Coriolis force is represented by $\epsilon_{\alpha\beta\gamma} f_3 U_{\beta s}$.

Moreover, the bottom shear stress in the hydrodynamic model was modified in order to take into account the wave-current interaction effects on the bottom roughness (CFW), following [9]'s theoretical framework.

To guarantee mass conservation, the mass transport induced by the Stokes drift in the depth-integrated continuity equation (5) was included. The overbar symbol denotes a depth-integrated variable.

$$\frac{\partial \bar{h}}{\partial t} + \frac{\partial \bar{h} \bar{u}_\alpha}{\partial x_\alpha} = - \frac{\partial \bar{h} \bar{U}_{as}}{\partial x_\alpha} \quad (5)$$

At the offshore open boundary, in the case of no other external forcing terms (such as tidal forces), two conditions are imposed for the phase-averaged elevation (6) and the horizontal velocities (7) [11]:

$$\hat{\eta} = - \frac{J}{g} \quad (6)$$

$$\bar{u}_\alpha = - \bar{U}_{as} \quad (7)$$

The momentum lost by waves due to depth-induced wave breaking (FDX, FDY) and bottom friction (FBX, FBY) is imposed in the hydrodynamic model as free surface and bottom stresses, respectively. The momentum lost by waves due to white-capping together with the input momentum transferred from wind to the wave field (FWX, FWY) is also imposed as a surface stress in the hydrodynamic model.

B. Implementation

In the following, we give a brief explanation on the way the coupled system works (Figure 1) [5]. Both TOMAWAC and TELEMAC-3D models run with the same horizontal mesh.

TELEMAC-3D starts the calculation. The Nikuradse roughness, the z-levels, and the computed depth-integrated velocities and mean surface elevation are communicated to TOMAWAC. In its turn, TOMAWAC computes, over a time step, the wave forcing terms: the Stokes drift components, the wave-induced pressure, the wave breaking and the bottom-induced dissipation momentum contributions. The last two terms are imposed as surface and bottom stresses,

respectively, in the hydrodynamic model. Furthermore, the wave model calculates the wave-enhanced vertical mixing coefficient v_{wz} that is added to the vertical turbulence viscosity in TELEMAC-3D. This process is repeated each time step or made within a coupling period defined by the user. The coupling period between TELEMAC-3D and TOMAWAC can be larger than the time step of the models. The time step of each of the models does not have to be the same, just a multiple of each other.

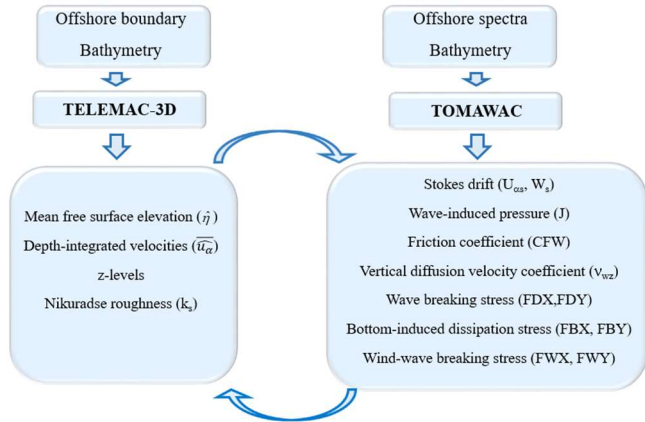


Figure 1 Scheme of the different terms computed and exchanged by TELEMAC-3D and TOMAWAC

C. Steering file: new key words

In order to compute a wave– current environment in a 3D framework, with the coupling system based in the vortex force formalism described above, the user must include the key word *COUPLING WITH: TOMAWACT3D* in the steering file. The existing coupling, where the radiation stresses are distributed uniformly over the depth, is then distinguished from the new developments.

If the user wants to include the momentum lost by waves due to bottom friction the key word BOTTOM FRICTION DUE TO WAVES must be set to TRUE in the steering file. Please be aware that this term shall be included only when the vertical resolution near the bottom in TELEMAC-3D is sufficiently refined.

Moreover the wave enhanced vertical mixing formulation follows [12] approach with the same parameters used in that paper. A sensitivity analysis would be advised if the wave enhanced vertical mixing is expected to have a predominant role in the 3D flow dynamics.

III. TEST CASE

In the present section the capability of the new coupled system to model rip currents is tested and the vertical structure of the flow is evidenced. The comparison of numerical results between the existing TELEMAC-3D - TOMAWAC coupling, based on the radiation stresses uniformly distributed over depth, and the new one, based on a vortex-force formalism is made.

A. Rip current

The present test-case is based on laboratory wave-basin experiment [10]. The bathymetry is made of two bars which

induce wave breaking and the generation of a rip current system. The wave basin is 17.2 m in the cross-shore direction and 18.7 m in the longshore direction. The slope is 1:5 from offshore up to three meters from the wave maker and then 1:30 till the end of the beach. The generated waves are monochromatic and perpendicular to the beach.

The same wave basin configuration was defined on the numerical model. The computational domain was discretized equally for both models with 0.2 m ix x- and y- directions (*Figure 2*). In TELEMAC-3D, 8 horizontal planes were distributed over depth.

The time step was set to $\Delta t = 0.03$ s for both hydrodynamic and wave models. Conditions (4) and (5) were assigned at the offshore boundary and walls were defined at lateral and shoreward boundaries. The Nikuradse roughness was set to $k_s = 0.01$ m. The $k-\epsilon$ model was the chosen turbulence model to compute the vertical turbulence viscosity. To take into account the wave-enhanced mixing in the hydrodynamic model due to wave breaking, the parameters $c_b = 0.03$ and $a_b = 1.2$ were used [12].

A value of $v_H = 1.10^{-2} \text{ m}^2\text{s}^{-1}$ was set for the horizontal turbulence viscosity and $v_z = 1.10^{-6} \text{ m}^2\text{s}^{-1}$. The numerical simulations with TOMAWAC were performed with spectral parameters that match the monochromatic laboratory experiments. This way, a significant wave height was set to $H_s = 0.067 \text{ m}$. The minimum frequency was set to 0.187 Hz, the number of frequencies to 7 and the frequential ratio to 1.4. The directional discretization was made through 24 direction bins. For the depth-induced breaking the model proposed by [12] was chosen with $\gamma_2 = 1.0$.

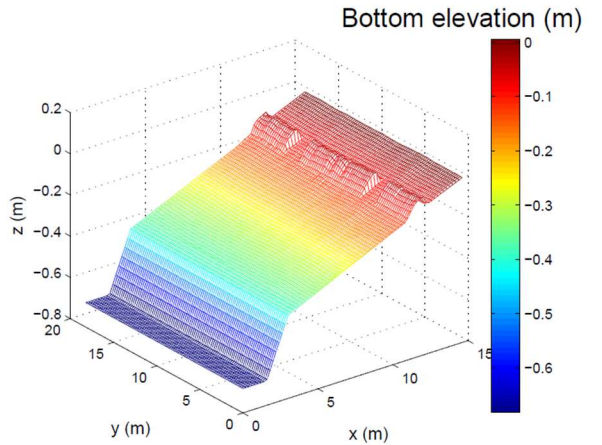


Figure 2 Wave basin bathymetry of the rip current test case

B. Results

The wave height evolution over the domain is of major importance to correctly obtain the flow pattern of a rip current system. In its turn the current field is going to have a significant role on the wave height evolution [10]. Therefore a great influence is also noticed on the rip currents from the interaction with waves.

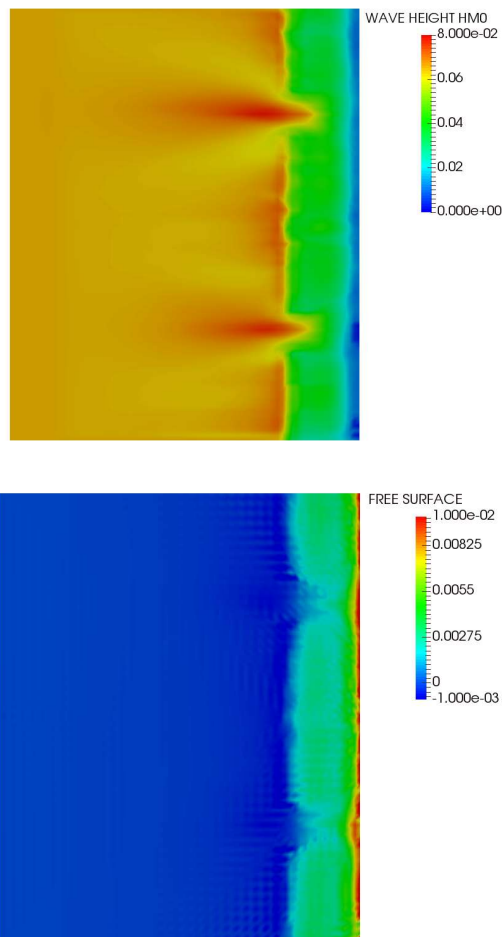


Figure 3 Wave height (m) and mean free surface elevation (m) patterns over the domain

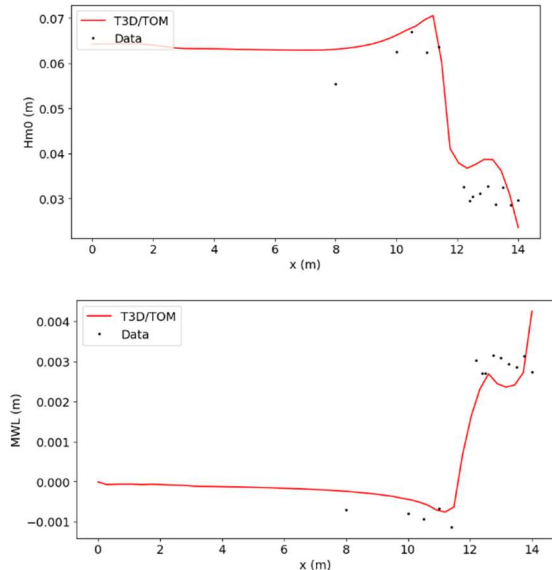


Figure 4 Cross-shore evolution of significant wave height (above) and mean water level (below) over the bar at $y = 9.2$ m. Comparison between numerical results (lines) and data (dots) from [14].

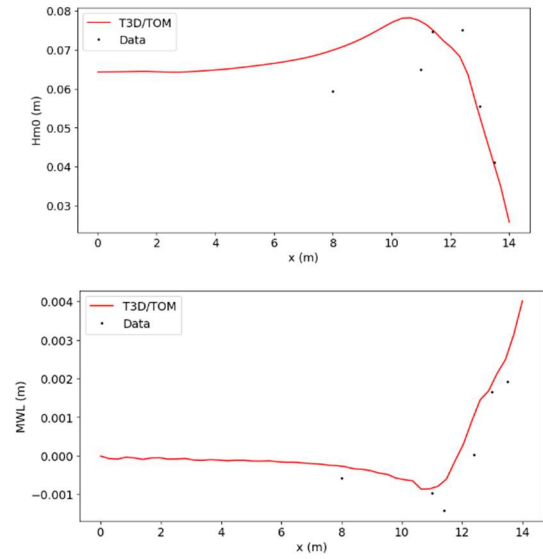


Figure 5 Cross-shore evolution of significant wave height (above) and mean water level (below) through the rip channel at $y = 13.6$ m. Comparison between numerical results (lines) and data (dots) from [14].

Due to bathymetry features, the wave pattern in the domain is quite different in the channel areas and over the bars (upper panel of *Figure 3*). The variation of the mean surface elevation (lower panel of *Figure 3*) alongshore induces longshore pressure gradients. The latter generate offshore oriented currents that converge into the rip channel and onshore oriented currents over the bar.

The breaking pattern reveals a quite distinct behaviour between the bar and the rip channel. While over the bars the waves break suddenly and then near the shoreline a second less intense breaking is observed, in the channel, due to the greater water depth, the waves break more progressively and penetrate further into the inshore zone of the channel, inducing a longshore current near the shoreline that flows away from the channel (*Figure 6*).

The comparison between numerical results and measurements of the significant wave height and mean water level over the bar (at $y = 9.2$ m) and through the rip channel ($y = 13.6$ m) are shown on *Figure 4* and *Figure 5* respectively. Over the bar the comparisons between the numerical simulations and data are similar. The waves break suddenly when encountering the bar and a sudden and significant rise of the water level occurs due to the strong wave breaking in this region. Through the rip channel, the coupled system reproduces quite well the progressive evolution of the wave set-up up to the shoreline but it shows some difficulties in reproducing the exact location where waves start to break through the rip channel. Possibly, the numerical opposing currents were to strong and induce the waves to break earlier than observed in the experiments.

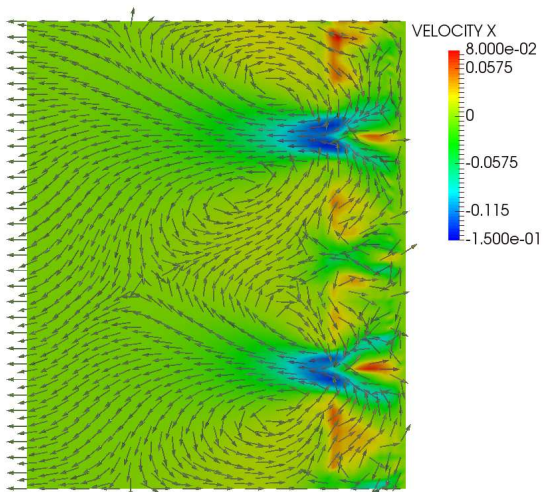


Figure 6 Depth integrated rip current (m/s) patterns over the domain

The vertical structure of the cross-shore and longshore currents is presented below in the longshore direction of the domain at $x = 11.6$ m.

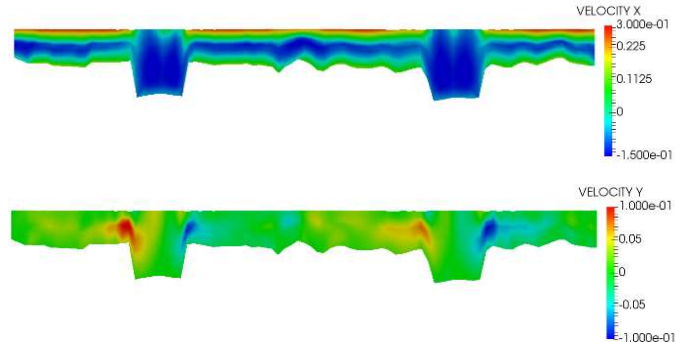


Figure 7 Alongshore variation of cross-shore and longshore current (m/s) components at $x = 11.6$ m

It can be seen a strong vertical shear of the quasi-Eulerian cross-shore velocity component above the bar crest. It increases from bottom to the free surface, being oriented towards the shoreline. When encountering the bars, waves break, and a strong mass flux occurs. This can be confirmed by the vertical distribution of the cross-shore component of the Stokes drift (upper panel of *Figure 8*).

Within the rip channels, the vertical profile of the cross-shore velocities is not so sheared, but it shows relatively high negative velocities approximately in the middle of the water column. Then it starts to slightly decrease in magnitude towards the free surface and the bottom.

The longshore components of the quasi-Eulerian velocity are one order of magnitude lower than the quasi-Eulerian cross-shore velocities. This is caused by the weak longshore component of the Stokes drift (lower panel of *Figure 8*). Even so, they present high variability along the longshore bars and channels. At least three inflection points for the velocities can be clearly identified: two in each channel and one over the bar. These inflection points are generated by the variability of the mean surface elevation in the longshore direction which

in its turn exists due to the spatial variability of the dissipation rate of the incident wave field.

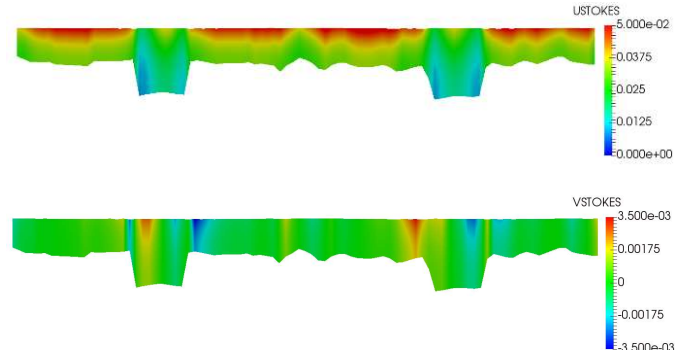


Figure 8 Alongshore variation of crossshore and longshore Stokes drift (m/s) components at $x = 11.6$ m

In the figures below we plot the evolution of cross-shore and longshore current components along two cross-shore directions of the domain ($y = 13.6$ m in the rip channel and $y = 9.2$ m over the bar).

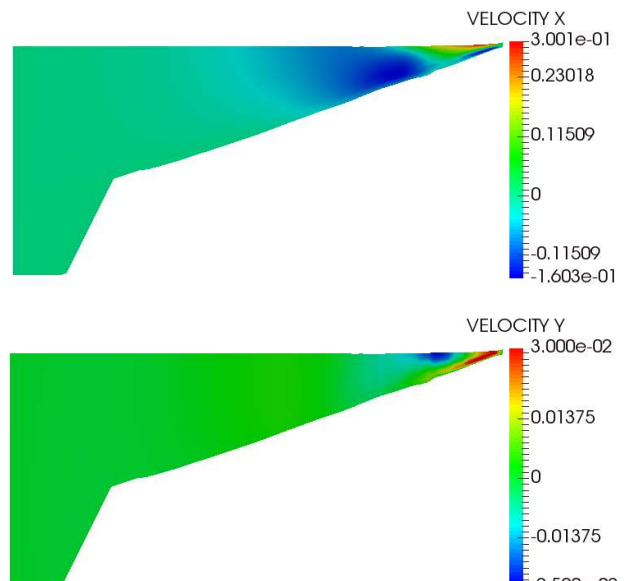
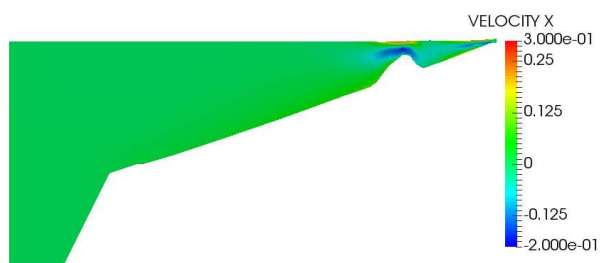


Figure 9 Crossshore variation of cross-shore and longshore current (m/s) components in the rip-channel at $y = 13.6$ m.



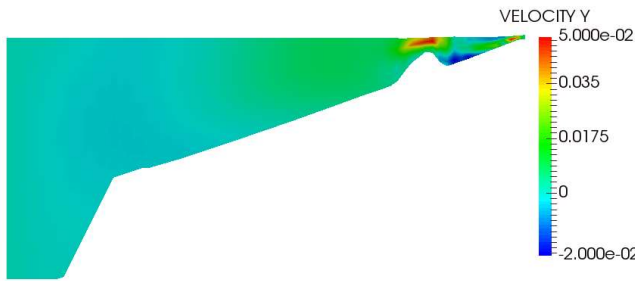


Figure 10 Crossshore variation of cross-shore and longshore current (m/s) components over the bar at $y = 9.2$ m

It can be seen that in both wave breaking locations there is a strong vertical shear of the cross-shore quasi-Eulerian velocity: near the free surface it is directed onshore while near the bottom an undertow is verified. When analysing the rip current through the rip channel the velocities oriented offshore are stronger than the ones observed over the bar.

One of the great advantages of the vortex force formalism to describe waves and current interactions is that the vortex force is clearly distinguished. Therefore it is possible to study the circulations and water motions in the mean flow. Moreover, within this approach, it is possible to show the distribution of the vortex force over the domain that in its turn contributes to the vortices located between the bar and the channel and near the shoreline.

If the radiation stress is assumed to be uniformly distributed over the depth, the vertical structure of the flow cannot be assessed. As it is shown above, there is an important vertical shear of the velocity at certain locations of the domain, which can strongly impact the morphodynamics in similar beach configurations.

IV. CONCLUDING REMARKS

The implementation of the coupled system between the three-dimensional flow model TELEMAC-3D and the spectral wave model TOMAWAC [4], [5] in the next official TELEMAC-MASCARET v8p1 version is presented. The capability of the new coupled system, based on a vortex force formalism, to represent rip currents on a barred beach is assessed and the vertical structure of the flow is analysed.

Other parametrizations and vertical distributions of the non-conservative wave forcing terms should be the subject of further research.

Moreover in the present work, the vertical current shear is ignored within the wave forcing terms, and the horizontal diffusion velocity coefficient was set by using a simple approach (imposing a constant value along the domain). The former feature should be included and different and more complex turbulence modelling approaches should be tested.

ACKNOWLEDGEMENT

Maria João Teles would like to acknowledge the support of a PhD grant (SFRH/BD/61269/2009) from FCT (Fundação para a Ciência e Tecnologia), Portugal. The

authors would also like to acknowledge all the support given by the TELEMAC-MASCARET development team.

REFERENCES

- [1] Longuet-Higgins, M. S., Stewart, R. W., "Radiation stress and mass transport in gravity waves, with applications to surf beats. Journal of Fluid Mechanics", 1962, Vol. 13, pp 481-504.
- [2] Hervouet J.-M., "Hydrodynamics of free surface flows, modelling with the finite element method. Editions Wiley & Sons." ISBN 978-0-470-03558, 2007, 342 p.
- [3] Benoit M., Marcos F., Becq F., "Development of a third generation shallow water wave model with unstructured spatial meshing. Proc. 25th Int. Conf. on Coastal Eng. (ICCE'1996)", 2-6 September 1996, Orlando (Florida, USA), pp 465-478.
- [4] Teles M.J., "Wave-current modelling at local and regional scales", PhD thesis, University of Lisbon, Instituto Superior Técnico, Lisbon, 2013.
- [5] Teles M.J., Pires-Silva A., Benoit M., "Computation of 3D coastal hydrodynamics through the vortex force formalism implemented by coupling. Proc. 21st TELEMAC MASCARET User Conference, 15th - 17th October, Grenoble", 2014, pp 11-17.
- [6] Andrews, D. G., McIntyre, M. E., "An exact theory of non linear waves on a Lagrangian mean flow." Journal of Fluid Mechanics, 1978a, Vol. 89, pp 609-646.
- [7] Arduhin F., Rasile N., Belibassakis K.A., "Explicit wave-averaged primitive equations using a generalized Lagrangian mean." Ocean Modelling, Vol. 20(1), 2008, pp 35-60.
- [8] Bennis A.-C., Arduhin F., Dumas F., "On the coupling of wave and three-dimensional circulation models: Choice of theoretical framework, practical implementation and adiabatic tests." Ocean Modelling, 2011, Vol. 40(3-4), pp 260-272.
- [9] Christoffersen, J. B., Jonsson, I. G., "Bed friction and dissipation in a combined current and wave motion." Ocean Engineering, 1985, Vol. 12, pp 387-949 423.
- [10] Haas, K. A., Svendsen, I. A., "Laboratory measurements of the vertical structure of rip currents". Journal of Geophysical Research, 2002, Vol. 107 (C5), 3047.
- [11] Rasile, N. "Impact of waves on the ocean circulation." PhD thesis, Université de Bretagne Occidentale, France, 2007.
- [12] Battjes, J.A. and Janssen, J.P.F.M., "Energy loss and set-up due to breaking of random waves." In Proc. 16th Int. Conf. Coastal Eng., pp 569-587, 1978.
- [13] Uchiyama, Y., McWilliams, J. C., Shchepetkin, A. F., "Wave-current interaction in an oceanic circulation model with a vortex-force formalism: Application to the surf zone". Ocean Modelling, 2010, Vol. 34, pp 16-35.
- [14] Haller, M. C., Dalrymple, R. A., Svendsen, I. A., "Experimental study of nearshore dynamics on a barred beach with rip channels". Journal of Geophysical Research, 2002 Vol.107 (C6), 3061.

